Plasticity Analysis of the Strain in the Tangential Direction of Solid Wood Subjected to Compression Load in the Longitudinal Direction

Hiroshi Yoshihara

Uniaxial compression tests in the grain (longitudinal) direction of solid wood were conducted using specimens of Sitka spruce and Japanese birch. The nonlinear stress-strain behavior was analyzed using plasticity theory, which is typically applied to ductile materials such as metals. The relationship between the longitudinal and tangential directions obtained from the experimental results showed nonlinearity, as predicted based on plasticity theory. Nevertheless, it was more pronounced in the experimental results than in the plasticity analysis.

Keywords: Compression test; Longitudinal strain; Material nonlinearity; Plasticity theory; Solid wood; Tangential strain

*Contact information: Faculty of Science and Engineering, Shimane University, Nishikawazu-cho 1060, Matsue, Shimane 690-8504, Japan; *Corresponding author: yosihara@riko.shimane-u.ac.jp*

INTRODUCTION

When solid wood is subjected to compression load, its stress-strain diagram is initially linear, and it successively demonstrates nonlinearity similar to that of ductile materials such as metals. After the nonlinearity is induced, the stress-strain relationship of solid wood should be described using a theory other than anisotropic elasticity, such as plasticity. Plasticity theory, the details of which are described below, was originally proposed to describe the deformation properties of metals (Hill 1950; Yamada 1980) with consideration of the microscopic crystalline structure. Additionally, it has been developed to describe the nonlinear stress-strain behaviors of non-metallic materials, such as concrete (Chen and Chang 1978; Cheng and Suzuki 1980; Chen *et al.* 1980). There are several examples of the application of plasticity theory to describe the macroscopically nonlinear stress-strain behaviors of solid wood, even though its microstructure is different from that of metals (Norris 1962; Zakic 1975; Tujino 1975, 1976; Okusa 1977, 1978; Yoshihara and Ohta 1992, 1994, 1996; Moses and Prion 2002, 2004; Mackenzie-Helnwein *et al.* 2003, 2005; Hong *et al.* 2011; Hering *et al.* 2012). Nevertheless, there have been few reports examining the validity of plasticity theory itself (Yoshihara and Ohta 1992, 1994; Mackenzie-Helnwein *et al.* 2003, 2005; Hering *et al.* 2012). In particular, it is difficult to find any examples discussing the relationship between the longitudinal and transverse strains in solid wood under uniaxial compression loading condition after the nonlinearity is induced. Examples examining the relationship between the longitudinal and transverse strains are often restricted to the discussion of the elastic condition related to Poisson's ratio (Taniguchi and Ando 2010a,b; Ando *et al.* 2013; Mascia and Vanalli 2012; Mascia and Nicolas 2013).

In this study, the longitudinal and tangential strains of Sitka spruce (*Picea sitchensis* Carr.) and Japanese birch (*Fagus crenata* Endl.) were measured during uniaxial compression loading in the longitudinal direction until the compressive stress reached its maximum. The stress-strain relationships in the post-elastic region were analyzed based on plasticity theory. By comparing the stress-strain relationships obtained from the compression test and plasticity analysis, it was determined whether the plasticity theory (mathematical theory of plasticity in this study) is applicable for describing the nonlinear stress-strain behavior about the longitudinal-tangential plane of Sitka spruce and Japanese birch.

STRESS-STRAIN RELATIONSHIP DERIVED FROM PLASTICITY THEORY

The stress-strain behavior of ductile material is often analyzed based on the mathematical theory of plasticity (Hill 1950). The plasticity theory adopted in this study is based on the small deformation of material. In the post-peak stress region, large deformation can involve the buckling and cracking of cell walls, and such phenomena cannot be described by the plasticity theory described below (Easterling *et al.* 1982; Ashby *et al.* 1985). From this point of view, the stress-strain behaviors in the post-peak stress region are not considered in this study.

In the plane stress condition, the relationship between the stress increment $\{d\sigma_{ij}\}$ and the strain increment $\{d\varepsilon_{ij}\}$ in the post-elastic region is represented as follows (Hill 1950; Yamada 1980),

$$\left\{d\sigma_{ij}\right\}=\begin{Bmatrix} d\sigma_x \\ d\sigma_y \\ d\tau_{xy} \end{Bmatrix}=\left[D^{\mathrm{e}}\right]\left\{d\varepsilon_{ij}\right\}-\left[D^{\mathrm{e}}\right]\left\{d\varepsilon_{ij}^{\mathrm{p}}\right\} \tag{1}$$

where $[D^{\mathrm{e}}]$ is the stiffness matrix in the elastic region and $\{d\varepsilon_{ij}{}^{\mathrm{p}}\}$ is the plastic strain increment. When Young's moduli in the x and y directions are defined as E_x and E_y, respectively, and Poisson's ratio and the shear modulus in the xy plane are defined as ν_{xy} and G_{xy}, respectively, $[D^{\mathrm{e}}]$ is obtained as follows:

$$\left[D^{\mathrm{e}}\right]=\begin{bmatrix} \dfrac{E_x^2}{E_x-E_y\nu_{xy}^2} & \dfrac{E_xE_y\nu_{xy}}{E_x-E_y\nu_{xy}^2} & 0 \\ \dfrac{E_xE_y\nu_{xy}}{E_x-E_y\nu_{xy}^2} & \dfrac{E_xE_y}{E_x-E_y\nu_{xy}^2} & 0 \\ 0 & 0 & G_{xy} \end{bmatrix}=\begin{bmatrix} d_{11} & d_{12} & 0 \\ d_{12} & d_{22} & 0 \\ 0 & 0 & d_{33} \end{bmatrix} \tag{2}$$

In this study, the x and y directions coincided with the longitudinal (grain) direction and tangential direction (direction parallel to the ring direction) of solid wood, respectively, and the compression load was applied in the *x* direction. According to the Prandtl-Reuss theory (Prandtl 1924; Reuss 1930), $\{d\varepsilon_{ij}^{\mathrm{p}}\}$ is derived as follows,

$$\left\{d\varepsilon_{ij}^{\mathrm{p}}\right\} = g\left\{\frac{\partial f}{\partial \sigma_{ij}}\right\}df = g\left\{\frac{\partial f}{\partial \sigma_{ij}}\right\}d\bar{\sigma} = \left\{\frac{\partial f}{\partial \sigma_{ij}}\right\}\overline{d\varepsilon^{\mathrm{p}}} \tag{3}$$

where *f* is the plastic potential, $\bar{\sigma}$ is the equivalent stress, $\overline{d\varepsilon^{\mathrm{p}}}$ is the equivalent plastic strain increment, and *g* is the inverse of the gradient of the $\bar{\sigma} - \overline{\varepsilon^{\mathrm{p}}}$ relationship. By substituting Eq. (3) into Eq. (1), the following results:

$$\left\{d\sigma_{ij}\right\} = \left[D^{\mathrm{e}}\right]\left\{d\varepsilon_{ij}\right\} - g\left[D^{\mathrm{e}}\right]\left\{\frac{\partial f}{\partial \sigma_{ij}}\right\}df \tag{4}$$

According to plasticity theory, *f* and $\bar{\sigma}$ are similar to a yield criterion. In this study, the yield criterion proposed by Hill (1950), the applicability of which has been verified in several previous studies (Yoshihara and Ohta 1992, 1994, 1996), was used, and it is derived as follows:

$$f = \bar{\sigma} = \sqrt{Q\left[\frac{\sigma_x^2}{X^2} + \frac{\sigma_y^2}{Y^2} + \frac{\tau_{xy}^2}{S^2} - \frac{\sigma_x \sigma_y}{X^2}\right]} \tag{5}$$

where *X* and *Y* are the yield stresses in the *x* and *y* directions, respectively, *S* is the yield shear stress in the *xy* plane, and *Q* is a constant with the dimension of $(\text{stress})^2$, such that the quantities *f* and $\bar{\sigma}$ also have the units of stress. In this study, *Q* is assumed to be equal to X^2, so *df* is obtained from Eqs. (1) and (4) as:

$$\begin{aligned} df &= \frac{\partial f}{\partial \sigma_x}d\sigma_x + \frac{\partial f}{\partial \sigma_y}d\sigma_y + \frac{\partial f}{\partial \tau_{xy}}d\tau_{xy} \\ &= \left\lfloor \frac{\partial f}{\partial \sigma_{ij}} \right\rfloor \left\{d\sigma_{ij}\right\} = \left\lfloor \frac{\partial f}{\partial \sigma_{ij}} \right\rfloor \left[D^{\mathrm{e}}\right]\left\{d\varepsilon_{ij}\right\} - g\left\lfloor \frac{\partial f}{\partial \sigma_{ij}} \right\rfloor \left[D^{\mathrm{e}}\right]\left\{\frac{\partial f}{\partial \sigma_{ij}}\right\}df \end{aligned} \tag{6}$$

Therefore,

$$df = \frac{\left\lfloor \frac{\partial f}{\partial \sigma_{ij}} \right\rfloor \left[D^{\mathrm{e}}\right]\left\{d\varepsilon_{ij}\right\}}{1 + g\left\lfloor \frac{\partial f}{\partial \sigma_{ij}} \right\rfloor \left[D^{\mathrm{e}}\right]\left\{\frac{\partial f}{\partial \sigma_{ij}}\right\}} \tag{7}$$

By substituting Eq. (7) into Eq. (4), the stress-strain relationship in the plastic region is derived as follows,

$$\{d\sigma_{ij}\} = \left([D^{e}] - \frac{[D^{e}]\left\{\frac{\partial f}{\partial \sigma_{ij}}\right\}\left\lfloor \frac{\partial f}{\partial \sigma_{ij}} \right\rfloor [D^{e}]}{\frac{1}{g} + \left\lfloor \frac{\partial f}{\partial \sigma_{ij}} \right\rfloor [D^{e}] \left\{\frac{\partial f}{\partial \sigma_{ij}}\right\}} \right) \{d\varepsilon_{ij}\} = [D^{p}]\{d\varepsilon_{ij}\} \tag{8}$$

where $[D^{p}]$ is the stiffness matrix in the plastic region. From Eq. (5), $\lfloor \partial f/\partial \sigma_{ij} \rfloor$ is derived as follows:

$$\left\lfloor \frac{\partial f}{\partial \sigma_{ij}} \right\rfloor = \frac{1}{2\bar{\sigma}} \lfloor \sigma_x' \quad \sigma_y' \quad \tau_{xy}' \rfloor \tag{9}$$

In this study, a uniaxial compression load was applied along the x direction, so $\sigma_y = \tau_{xy} = 0$. Therefore,

$$\begin{cases} \sigma_x' = Q\left(\dfrac{2\sigma_x}{X^2} - \dfrac{\sigma_y}{X^2}\right) = 2\sigma_x \\ \sigma_y' = Q\left(\dfrac{2\sigma_y}{Y^2} - \dfrac{\sigma_x}{X^2}\right) = -\sigma_x \\ \tau_{xy}' = Q\dfrac{2\tau_{xy}}{S^2} = 0 \end{cases} \tag{10}$$

The quantity $[D^{p}]$ then is derived from Eqs. (8) through (10) as,

$$[D^{p}] = [D^{e}] - \frac{1}{S}\begin{bmatrix} S_1^2 & S_1S_2 & 0 \\ S_1S_2 & S_2^2 & 0 \\ 0 & 0 & 0 \end{bmatrix} \tag{11}$$

where

$$\begin{cases} S_1 = d_{11}\sigma_x' + d_{12}\sigma_y' \\ S_2 = d_{12}\sigma_x' + d_{22}\sigma_y' \end{cases} \tag{12}$$

and

$$S = \frac{4\bar{\sigma}^2}{g} + S_1\sigma_x' + S_2\sigma_y' \tag{13}$$

To determine the stiffness matrix $[D^p]$, it is necessary to derive the value of g. The g value can be obtained from the stress-plastic strain relationship in the loading direction, σ_x-ε_x^p. The plastic strain ε_x^p is obtained by subtracting the elastic strain component, which can be derived as σ_x/E_x, from the total strain ε_x as follows:

$$\varepsilon_x^p = \varepsilon_x - \frac{\sigma_x}{E_x} \tag{14}$$

From Eqs. (4) through (6), $\bar{\sigma} = \sigma_x$ and $\overline{d\varepsilon^p} = d\varepsilon_x^p$ in the uniaxial condition ($\sigma_x \neq 0$, $\sigma_y = \tau_{xy} = 0$). The σ_x-ε_x^p relationship is derived by the following equation, which was proposed by Ludwik (Hill 1950):

$$\sigma_x = X + K\left(\varepsilon_x^p\right)^n \tag{15}$$

where n and K are the material's parameters obtained by the regression of σ_x-ε_x^p relationship. The $\bar{\sigma} - \overline{\varepsilon^p}$ relationship is derived as $\bar{\sigma} = X + K\left(\overline{\varepsilon^p}\right)^n$, similarly to Eq. (15). Therefore, $1/g$ is obtained from Eqs. (5) and (19) as follows:

$$\frac{1}{g} = \frac{d\bar{\sigma}}{\overline{d\varepsilon^p}} = nK\left(\overline{\varepsilon^p}\right)^{n-1} \tag{16}$$

EXPERIMENTAL

Specimens

Sitka spruce (*Picea sitchensis* Carr.) and Japanese birch (*Fagus crenata* Endl.) were investigated. The densities of these lumbers at 12% moisture content (MC) were 373 ± 2 and 587 ± 3 kg/m^3, respectively. These lumber samples were free of defects, such as knots or grain distortions, so specimens cut from them could be regarded as "small and clear".

The samples were stored at a constant 20 ºC and 65% relative humidity (RH) before and during the test, so the specimens were confirmed to be in an air-dried condition. The moisture content of the specimens was 11.7± 0.2%. The room temperature and RH were maintained throughout the tests.

The lumber was sawn into several boards with thicknesses of 45 mm, and the specimens were then cut from these plates. The specimens were long-matched and they had dimensions of 60 (L) × 30 (R) × 30 (T) mm^3. The dimensions of the specimens were determined according to JIS Z2101-2009. Figure 1 shows the photograph of the cross-section of the specimens. As shown in the photograph, the annual ring orientation could be ignored and its orthotropic symmetry was confirmed. Ten specimens were used for each species.

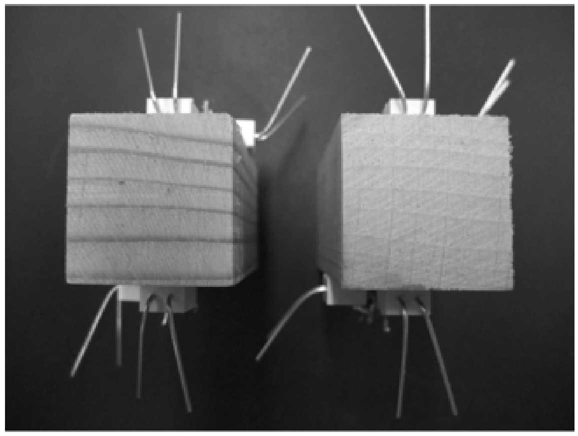

Fig. 1. Photograph of the cross-section of the specimen used in the experiment. Left: Sitka spruce, Right: Japanese birch

Compression Tests

To measure the normal strain in the longitudinal and tangential directions of each specimen, ε_L and ε_T, a biaxial strain gage (Tokyo Sokki FCA-2-11, gage length = 2 mm) was bonded at both centers of the longitudinal-tangential plane. The ε_L and ε_T values were obtained by averaging the strain gage outputs detected from both planes. The specimen was set on a steel plate, and a compression load, P, was applied to the specimen with a cross-head speed of 0.5 mm/min until the load markedly decreased. The cross-head speed was determined such that the strain rate effect was not significant (Okuyama and Asano 1970).

The data of the load and strains were simultaneously recorded using a data logger (Tokyo Sokki TDS-303) at an interval of 2 sec. The total testing time was approximately 5 min. To prevent the bending moment induced at the end of the specimen, the compression plate was equipped with a spherical coupling, which allows the free rotation of the plate (Yoshihara and Yamamoto 2001) as shown in Fig. 2. Solid wood cannot be a perfectly homogeneous material, so inhomogeneous loading is easily induced based on various factors such as the density profile and distorted cutting in the specimen.

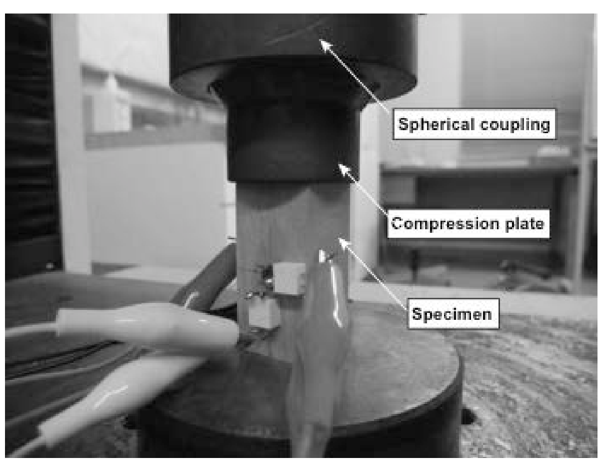

Fig. 2. Setup of the uniaxial-compression test

When considering these phenomena, it is difficult to compute the compressive stress while considering the inhomogeneity in the specimen. In this study, the load was assumed to be applied homogeneously to the specimen, and the compressive stress σ_L was obtained by dividing *P* by the cross sectional area *A*, whereas the longitudinal and transverse strains, ε_L and ε_T, respectively, were obtained by averaging the strain data obtained from both planes.

Figure 3(a) shows the definitions of Young's modulus, Poisson's ratio, and compressive strength, E_L, ν_{LT}, and σ_{max}, respectively, whereas Fig. 3(b) shows the definitions of secant modulus and secant Poisson's ratio, E_{sec} and ν_{sec}, respectively, the details of which are described below. The Young's modulus E_L and Poisson's ratio ν_{LT} were obtained from the initial slope of the σ_L-ε_L and ε_T-ε_L relationships, respectively. The compressive strength σ_{max} was determined from the maximum stress. The proportional limit stress σ_{pl} was obtained from the stress at the onset of nonlinearity in the σ_L-ε_L relationship. There are several methods to determine the proportional limit stress (Davies *et al.* 2001). In this study, it was determined from the stress where the half-thickness of the plotter trace deviated from the straight line drawn in the elastic region ($\sigma_L = E_L\varepsilon_L$) of the σ_L-ε_L relationship, as shown in Fig. 4 (Davies *et al.* 2001).

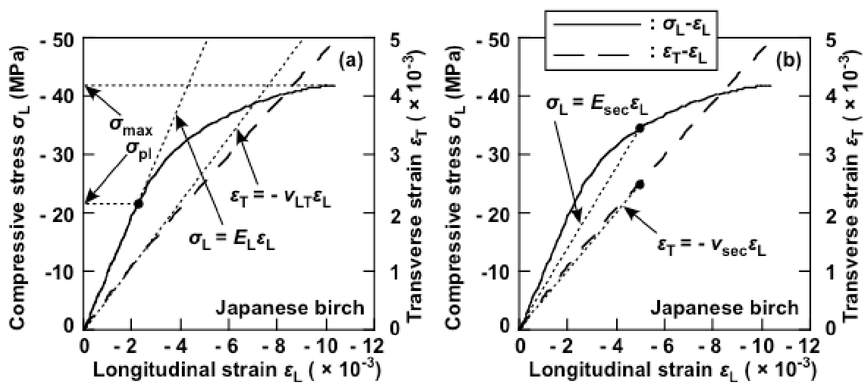

Fig. 3. (a) The definitions of Young's modulus, Poisson's ratio, and compressive strength, E_L, ν_{LT}, and σ_{max}, respectively, and (b) the definitions of secant modulus and secant Poisson's ratio in the nonlinear region, E_{sec} and ν_{sec}, respectively

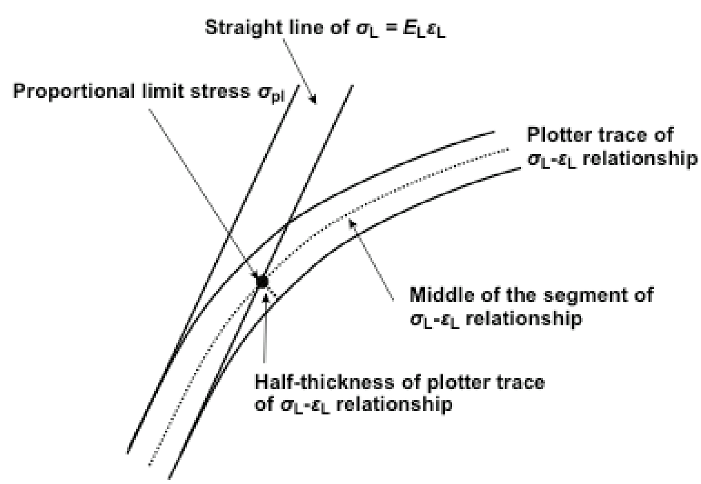

Fig. 4. Method of determination of the proportional limit stress σ_{pl}

Using Eq. (14), the plastic strain ε_L^p was obtained, and the parameters n and K were calculated by regressing the σ_L-ε_L^p relationship into Eq. (15). Note that σ_L, ε_L, E_L, ν_{LT}, and σ_{pl} obtained from the actual compression test correspond to σ_x, ε_x, E_x, ν_{xy}, and X in the plasticity analysis detailed in the previous section.

Plasticity Analysis

The stress-strain relationships in the nonlinear region were analyzed based on the plasticity theory by applying the following procedure:

(i) The stress and strain components and stiffness matrix at the stage k, $\{\sigma_{ij}\}_k$, $\{\varepsilon_{ij}\}_k$, and $[D^p_k]$, were assumed to be known.

(ii) In this study, a compression load was applied in the longitudinal direction alone. Therefore, Eq. (1) was simplified to

$$\left\{d\sigma_{ij}\right\} = \left\{\begin{matrix} d\sigma_x \\ 0 \\ 0 \end{matrix}\right\} \tag{17}$$

In this study, the value of $d\sigma_x$ was determined to be a constant value, *i.e.*, 0.1 MPa. From Eq. (8), the component of the strain increment at the stage (k + 1), $\{d\varepsilon_{ij}\}_{k+1}$, was obtained as follows:

$$\left\{d\varepsilon_{ij}\right\}_{k+1} = \left[D_k^p\right]^{-1}\left\{d\sigma_{ij}\right\} \tag{18}$$

(iii) The stress and strain components at the stage (k + 1) were obtained as follows:

$$\begin{cases} \left\{\sigma_{ij}\right\}_{k+1} = \left\{\sigma_{ij}\right\}_k + \left\{d\sigma_{ij}\right\} \\ \left\{\varepsilon_{ij}\right\}_{k+1} = \left\{\varepsilon_{ij}\right\}_k + \left\{d\varepsilon_{ij}\right\}_{k+1} \end{cases} \tag{19}$$

(iv) The process from (i) to (iii) was repeated until the σ_x value reached σ_{max}. The σ_x-ε_x and ε_y-ε_x relationships obtained from this procedure were compared with the σ_L-ε_L and ε_T-ε_L relationships obtained from the actual compression test.

RESULTS AND DISCUSSION

Figure 5 shows the compressive stress-longitudinal strain and transverse strain-longitudinal strain relationships, σ_L-ε_L and ε_T-ε_L, respectively. Figure 6 shows the photograph of the specimens obtained after the compression loading. As shown in Fig. 6, macroscopic fractures could not be found in the specimen until the compressive stress reached its maximum.

Table 1 lists the mechanical properties of Sitka spruce and Japanese birch obtained from the compression tests. In the plasticity analysis, however, the test data listed in Table 2, which were obtained from a single specimen, were used instead of the properties shown in Table 1. The σ_x-ε_x and ε_y-ε_x relationships obtained from the plasticity analysis were compared with the actual σ_L-ε_L and ε_T-ε_L relationships. The E_x, ν_{xy}, X, σ_{max}, ε_{max}, n, and K values were obtained from the actual compression tests conducted in this experiment, whereas the E_y values of Sitka spruce and Japanese birch were obtained from Hearmon (1948) and Forestry and Forest Products Research Institute, Japan (2004), respectively. Although the E_y value was required for the analysis, it did not influence the σ_x-ε_x and ε_y-ε_x relationships in this loading condition.

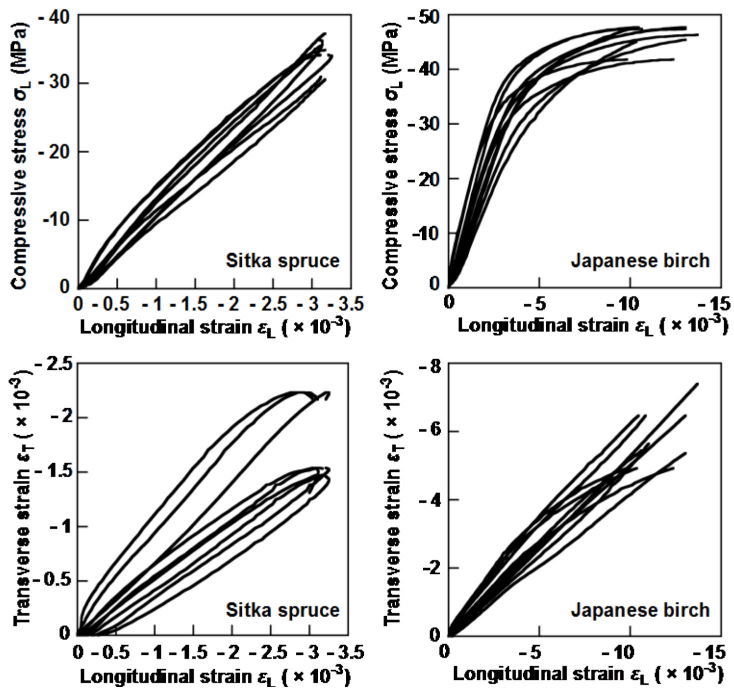

Fig. 5. Compressive stress-longitudinal strain and transverse strain-longitudinal strain relationships, σ_L-ε_L and ε_T-ε_L, respectively

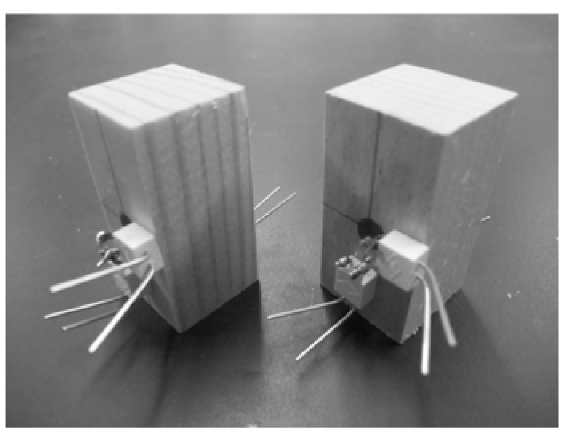

Fig. 6. Specimens obtained after compression loading. Left: Sitka spruce. Right: Japanese birch

Table 1. Mechanical Properties Obtained from the Compression Tests

	E_L (GPa)	ν_{LT}	σ_{pl} (MPa)	σ_{max} (MPa)	ε_{max}	n	K (GPa)
Sitka spruce	12.0 (1.3)	0.621 (0.051)	17.0 (1.9)	35.3 (1.1)	0.0033 (0.0004)	0.851 (0.086)	7.41 (2.60)
Japanese birch	10.9 (1.0)	0.543 (0.013)	24.7 (1.6)	46.2 (2.5)	0.0126 (0.0019)	0.407 (0.099)	0.22 (0.09)

Results are averages (SD). Parameters n and K are obtained by regressing the σ_L-ε_L^p relationship into Eq. (15). Ten specimens were used for each species.

Table 2. Mechanical Properties Used for the Plasticity Analysis Shown in Fig. 7

	E_x (GPa)	E_y (GPa)	ν_{xy}	X (MPa)	n	K (GPa)
Sitka spruce	13.1	0.39	0.520	13.0	35.0	0.79
Japanese birch	9.80	1.00	0.554	22.0	46.0	0.54

The secant modulus E_{sec} and secant Poisson's ratio ν_{sec} in the nonlinear region are defined using the temporary stress and strains as σ_L/ε_L and - $\varepsilon_T/\varepsilon_L$, respectively, as shown in Fig. 3(b). Figure 7 shows typical examples of the E_{sec}-ε_L and ν_{sec}-ε_L relationships obtained from the actual compression test and plasticity analysis conducted using the data listed in Table 2. As shown in Fig. 5, the nonlinear region in the σ_L-ε_L relationship for Japanese birch is significantly larger than that of Sitka spruce. Nonlinearity clearly exists in the ε_T-ε_L relationship, although it is less significant than that in the σ_L-ε_L relationship. When the σ_L-ε_L and ε_T-ε_L relationships are absolutely linear, the E_{sec} and ν_{sec} values coincide with the E_L and ν_{LT} values, respectively, throughout the ε_L range. In Fig. 7, however, it is clear that nonlinearity is significant in the σ_L-ε_L and ε_T-ε_L relationships obtained from the experimental results and the plasticity analysis for both species. Therefore, plasticity theory may be effective for predicting the tangential strain in the nonlinear region in this loading condition, even if the deformation mechanism is essentially different from that of metals. For both species, however, the nonlinearity in the ε_T-ε_L relationship obtained from the experimental result is more pronounced than that predicted from the plasticity analysis. Therefore, the ν_{sec} value at the maximum compressive stress σ_{max} experimentally obtained is smaller than that obtained from the plasticity analysis, as shown in Table 3. According to several previous studies, transverse cracking and splitting reduces the increasing rate of transverse strain (Surgeon *et al.* 1999; Kashtalyan and Soutis 2000; Pidaparti and Vogt 2002; Amara *et al.* 2005; Yoshihara and Tsunematsu 2007a, b). In addition to the reduction of transverse strain predicted from plasticity theory, the damage to the cell wall may enhance the reduction of the transverse strain. Microscopic observations during the compression loading may effectively reveal the influence of the plastic deformation and damage propagation. Although microscopic observations have been conducted in several previous studies (Easterling *et al.* 1982; Ashby *et al.* 1985), it should be conducted more carefully, particularly paying attention to the deformation in the transverse direction. Additionally, the compression plate was equipped with a hinge to prevent the bending moment induced at the end of the specimen. Nevertheless, it was difficult to reduce the distortion and frictional force at the end of the specimen entirely, so the load may not have been applied perfectly along the loading axis. This issue might enhance the nonlinearity in the transverse strain-longitudinal strain relationship obtained from the experimental result. Further research should also be conducted on the influence of the loading eccentricity on the transverse strain.

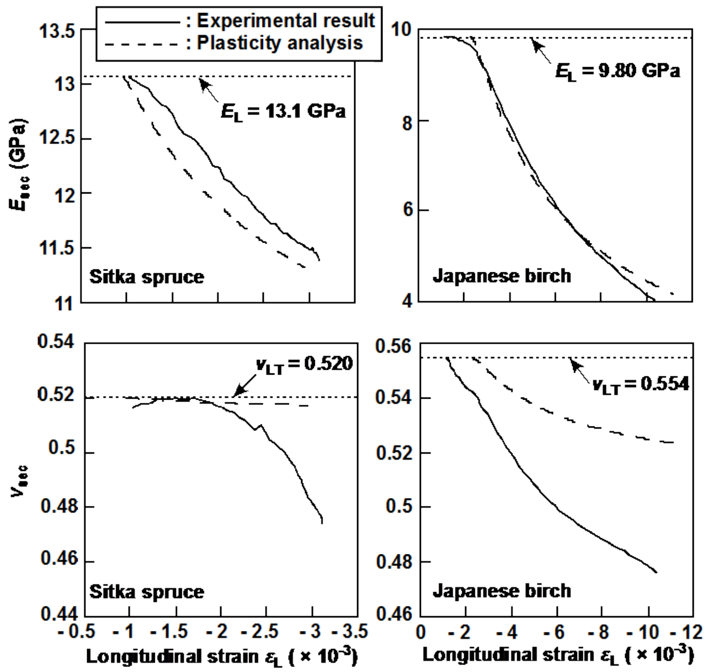

Fig. 7. The E_{sec}-ε_L and ν_{sec}- ε_L relationships obtained from the compression test and plasticity analysis

Table 3. E_{sec} and ν_{sec} Values of the Maximum Compressive Stress σ_{max} Obtained from the Compression Test and Plasticity Analysis

	E_{sec} (GPa)		ν_{sec}	
	Compression test	Plasticity analysis	Compression test	Plasticity analysis
Spruce	10.6 ± 1.6	10.5 ± 1.5	0.535 ± 0.043	0.590 ± 0.037
Japanese birch	3.75 ± 0.68	3.73 ± 0.61	0.495 ± 0.016	0.519 ± 0.018

Results are averages ± SD.

CONCLUSIONS

1. Similar to the compressive stress-longitudinal strain relationship, the tangential strain-longitudinal strain relationship showed nonlinearity, which was more pronounced in the experimental result than in the plasticity analysis.

2. Implicit damage might enhance the nonlinearity in the tangential strain-longitudinal strain relationship in addition to that predicted by plasticity theory.
3. Microscopic observation during compression loading may effectively reveal the source of nonlinearity in more detail.

ACKNOWLEDGMENTS

This work was supported in part by a Grant-in-Aid for Scientific Research (C) (No. 24580246) of the Japan Society for the Promotion of Science.

REFERENCES CITED

Amara, K. H., Tounsi, A., and Benzair, A. (2005). "Transverse cracking and elastic properties reduction in hygrothermal aged cross-ply laminates," *Mater. Sci. Eng. A* 396(1-2), 369-375.

Ando, K., Mizutani, M., Taniguchi, Y., and Yamamoto H. (2013). "Time dependence of Poisson's effect in wood III: Asymmetry of three-dimensional viscoelastic compliance matrix of Japanese cypress," *J. Wood Sci.* 59(4), 290-298.

Ashby, M. F., Easterling, K. E., Harrysson, R., and Maiti, S. K. (1985). "The fracture and toughness of woods," *Proc. Roy. Soc. A* 398(1815), 261-280.

Chen, W. F., and Chang, T. Y. P. (1978). "Plasticity solutions for concrete splitting tests," *J. Eng. Mech. Div. ASCE* 104(3), 691-704.

Chen, W. F., and Suzuki, H. (1980). "Constitutive models for concrete," *Comput. Struct.* 12(1), 23-32.

Chen, W. F., Suzuki, H., and Chang, T. Y. P. (1980). "Nonlinear analysis of concrete cylinder structures under hydrostatic loading," *Comput. Struct.* 12(4), 559-570.

Davies, P., Blackman, B. R. K., and Brunner, A. J. (2001). "Mode II delamination," in: *Fracture Mechanics Testing Methods for Polymers, Adhesive and Composites*, D. R. Moore, A. Pavan, and J. G. Williams (eds.), Elsevier, Amsterdam.

Easterling, K. E., Harrysson, R., Gibson, L. J., and Ashby, M. F. (1982). "On the mechanics of balsa and other woods," *Proc. Roy. Soc. A* 383(1784), 31-41.

Forestry and Forest Products Research Institute, Japan (2004). "Wood industry handbook," Maruzen, Tokyo.

Hearmon, R. F. S. (1948). "Elasticity of wood and plywood," HM Stationary Office, London.

Hering, S., Saft, S., Resch, E., Niemz, P., and Kaliske, M. (2012). "Characterisation of moisture-dependent plasticity of beech wood and its application to a multi-surface plasticity model," *Holzforschung* 66(3), 373-380.

Hill, R. (1950). *The Mathematical Theory of Plasticity*, Oxford University Press, London.

Hong, J. P., Barrett, J. D., and Lam, F. (2011). "Three-dimensional finite element analysis of the Japanese traditional post-and-beam connection," *J. Wood Sci.* 57(2), 119-125.

Kashtalyan, M., and Soutis, C. (2000). "Stiffness degradation in cross-ply laminates damaged by transverse cracking and splitting," *Composites A* 31(4), 335-351.

Mackenzie-Helnwein, P., Eberhardsteiner, J., and Mang, M. A. (2003). "A multi-surface plasticity model for clear wood and its application to the finite element analysis of structural details," *Comput. Mater.* 31(1-2), 204-218.

Mackenzie-Helnwein, P., Eberhardsteiner, J., and Mang, M. A. (2005). "Rate-independent mechanical behavior of biaxially stressed wood: Experimental observations and constitutive modeling as an orthotropic two-surface elasto-plastic material," *Holzforschung* 59(3), 311-321.

Mascia, N. T., and Vanalli, L. (2012). "Evaluation of the coefficients of mutual influence of wood through off-axis compression tests," *Construct. Build. Mater.* 40, 522-528.

Mascia, N. T., and Nicolas, E. A. (2013). "Determination of Poisson's ratios in relation to fiber angle of a tropical wood species," *Construct. Build. Mater.* 41, 691-696.

Moses, D. M., and Prion, H. G. L. (2002). "Anisotropic plasticity and the notched wood shear block," *Forest Prod. J*. 52(6), 43-54.

Moses, D. M., and Prion, H. G. L. (2004). "Stress and failure analysis of wood composites: A new model," *Composites B* 35(3), 251-261.

Norris, C. B. (1962). "Strength of orthotropic materials subjected to combined stresses," *Forest Prod. Lab. Rep.* 1816, 1-40.

Okusa, K. (1977). "On the prismatical bar torsion of wood as elastic and plastic material with orthogonal anisotropy," *Mokuzai Gakkaishi* 23(5), 217-227.

Okusa, K. (1978). "Studies on the shearing of wood especially on the elastic-plastic theory and fracture mechanics," *Bull. Fac. Agr. Kagoshima Univ.* 16, 21-61.

Okuyama, T., and Asano, I. (1970). "Effect of strain rate on mechanical properties of wood I. On the influence of strain rate to compressive properties parallel to the grain of wood," *Mokuzai Gakkaishi* 16(1), 15-19.

Pidaparti, R. M., and Vogt, A. (2002). "Experimental investigation of Poisson's ratio as a damage parameter for bone fatigue," *J. Biomed. Mater. Res.* 59(2), 282-287.

Prandtl, L. (1924). "Spannungsverteilung in plastischen kœrpern," *Proc.1st Int. Cong. Appl. Mech.*, Delft, pp. 43-54.

Reuss, E. (1930). "Beruecksichtigung der elastischen formaenderungen in der plastizitaetstheorie," *Z. Angew. Math. Mech.* 10(3), 266-274.

Surgeon, M., Vanswijgenhoven, E., Wevers, M., and van der Biest, M. (1999). "Transverse cracking and Poisson's ratio reduction in cross-ply carbon fibre-reinforced polymers," *J. Mater. Sci.* 34(22), 5513-5517.

Taniguchi, Y., and Ando, K. (2010). "Time dependence of Poisson's effect in wood. I: The lateral strain behavior," *J. Wood Sci.* 56(2), 100-106.

Taniguchi, Y., and Ando, K. (2010). "Time dependence of Poisson's effect in wood. II: Volume change during uniaxial tensile creep," *J. Wood Sci.* 56(4), 350-354.

Tujino, T. (1975). "Elastic-plastic analysis of the wooden plate. I. The case of simple compression under conditions without buckling of the nara band plate with a central hole," *Mokuzai Gakkaishi* 21(5), 265-272.

Tujino, T. (1976). "Elastic-plastic analysis of the wooden plate.II. Simple compression under conditions without buckling of the nara band plate with a reinforced opening," *Mokuzai Gakkaishi* 22(9), 481-487.

Yamada, Y. (1980). *Plasticity and Viscoelasticity*, Baifu-kan, Tokyo.

Yoshihhara, H., and Ohta, M. (1992). "Stress-strain relationship of wood in the plastic region I. Examination of the applicability of plasticity theories," *Mokuzai Gakkaishi* 38(8), 759-763.

Yoshihhara, H., and Ohta, M. (1994). "Stress-strain relationship of wood in the plastic region II. Formulation of the equivalent stress-equivalent plastic strain relationship," *Mokuzai Gakkaishi* 40(3), 263-267.

Yoshihhara, H., and Ohta, M. (1996). "Simulation of fracturing process of wood by finite element method," *Mater. Sci. Res. Int.* 2(3), 173-180.

Yoshihhara, H., and Ohta, M. (1997). "Stress-strain relationship of wood in the plastic region. III. Determination of the yield stress by formulating the stress-plastic strain relationship," *Mokuzai Gakkaishi* 43(6), 464-469.

Yoshihara, H., and Tsunematsu, S. (2007). "Bending and shear properties of compressed Sitka spruce," *Wood Sci. Technol.* 41(2), 117-131.

Yoshihara, H., and Tsunematsu, S. (2007). "Elastic properties of compressed spruce with respect to its cross section obtained under various compression ratios," *Forest Prod. J.* 57(4), 98-100.

Yoshihara, H., and Yamamoto, D. (2003). "Examination of compression testing methods for wood in the parallel to the grain direction," *Forest Prod. J.* 54(11), 56-60.

Zakic, B. D. (1975). "Inelastic behavior of wood beam-columns," *J. Struct. Div. ASCE* 101(2), 417-435.

Article submitted: October 11, 2013; Peer review completed: December 14, 2013; Revised version received and accepted: December 20, 2013; Published: January 6, 2014.